Suppression of *p-f* mixing and formation of a superzone gap in $CeSbNi_x$

M. H. Jung, D. T. Adroja,* N. Kikugawa, and T. Takabatake
Department of Quantum Matter, ADSM, Hiroshima University, Higashi-Hiroshima 739-8526, Japan

I. Oguro
Institute for Solid State Physics, University of Tokyo, Kashiwa 277-8581, Japan

S. Kawasaki and K. Kindo
Research Center for Materials Science at Extreme Conditions, Osaka University, Toyonaka 560-8531, Japan
(Received 4 January 2000; revised manuscript received 7 July 2000)

We report electrical resistivity, Hall coefficient, magnetic susceptibility, magnetization, and magnetoresistance measurements on $CeSbNi_x$ ($0 \leqslant x \leqslant 0.4$), where the Ni atoms are incorporated interstitially into the cubic cell of CeSb. The Néel temperature T_N drops from 16 K for $x=0$ to 9 K for $x=0.05$ and then gradually increases to 12.5 K for $x=0.4$. The initial depression of both T_N and saturation moment is ascribed to the collapse of *p-f* mixing by the decrease of the $5p$-hole concentration in the semimetallic CeSb. The resistivity for $x \geqslant 0.08$ shows a sharp rise just below T_N, which is quenched by the application of magnetic fields higher than the metamagnetic transition field. This finding indicates that a superzone gap is formed in the $5d$-electron band of $CeSbNi_x$ for $x \geqslant 0.08$ as a result of the type-I antiferromagnetic order.

Cerium monopnictides CeX (X=P, As, Sb, Bi) are antiferromagnets with low-density carriers. They have long been studied experimentally and theoretically,[1–3] because of their unusual magnetic properties such as complex magnetic phase diagram,[4] large magnetic anisotropy,[5] small crystal-field splitting,[6] etc., in spite of the simple NaCl-type structure. It has been shown that the magnetic properties of CeSb are very sensitive to any perturbation such as application of pressure[7,8] and partial substitution.[9–12] For example, the substitution of Te for Sb in CeSb by only 5% results in a large drop of the Néel temperature T_N from 16 to 4 K.[10,12] This is accompanied by a substantial decrease in the saturation moment from 2.1 to $0.7\mu_B$/Ce and an increase in the crystal-field splitting Δ from 37 to 49 K,[1,11] where Δ is the energy splitting from the ground-state doublet Γ_7 to the excited-state quartet Γ_8 of Ce^{3+} ion. These observations were explained by taking account of nonlinear *p-f* mixing between the $5p$-hole valence band of Sb and the $4f(\Gamma_8)$ state of Ce, as follows.[13,14] The Te atoms substituting for Sb have additional $5p$ electrons which should fill the $5p$-hole band of semimetallic CeSb. This in turn weakens the *p-f* mixing and causes significant effects on the physical properties mentioned above.

Recently, we have reported that Ni atoms can be incorporated interstitially into CeSb with keeping the cubic structure intact up to the solubility limit of $x=0.4$ in the formula $CeSbNi_x$.[15] For a single crystal of $x=0.15$, the magnetic susceptibility reveals an antiferromagnetic (AF) order at $T_N = 9.5$ K. The magnetization isotherm at 1.5 K shows a metamagnetic transition at 6.4 T with neither hysteresis nor anisotropy. The disappearance of complex and anisotropic nature in the magnetic properties suggested that the *p-f* mixing in CeSb is strongly reduced by the Ni incorporation. These observations are analogous to those in $CeSb_{1-y}Te_y$, mentioned above. The mechanism of the collapse of *p-f* mixing in $CeSbNi_x$ remains to be examined by the careful study of magnetic and transport properties using well characterized samples with different values of x. In the present paper, we report such measurements on a single crystal of $CeSbNi_{0.15}$ and polycrystalline samples of $CeSbNi_x$ ($0 \leqslant x \leqslant 0.4$). The effects of Ni incorporation will be discussed by comparing with those of the substitution of Te for Sb.

Polycrystalline samples of $CeSbNi_x$ with $x=0$, 0.02, 0.035, 0.05, 0.08, 0.15, 0.25, 0.35, and 0.40 were synthesized by arc melting. Electron-probe microanalysis indicated that the impurity phases of $CeNiSb_2$, $CeNi_2Sb_2$, and $CeNi_3$ were less than a few vol %.[15] X-ray powder-diffraction analysis showed that the cubic lattice parameter a increases almost linearly with x, at a rate $da/dx = 0.085$ Å. The method of the growth of single crystal $CeSbNi_{0.15}$ was described in Ref. 15. The magnetic susceptibility $\chi = M/B$ was measured in a field of 0.5 T in the temperature range 2–300 K. Hall effect was measured by the use of the conventional four-probe dc method in a field of 1 T. Measurements of electrical resistivity $\rho(T)$ were done by a standard four-probe dc technique for $1.3 \leqslant T \leqslant 300$ K and $B \leqslant 15$ T. Magnetization curves were recorded up to 15 T by an extraction method.

The temperature dependence of χ for all the samples of $CeSbNi_x$ ($0 \leqslant x \leqslant 0.4$) was found to obey the Curie-Weiss law at temperatures above 60 K. The effective magnetic moment $\mu_{\rm eff}$ is essentially independent of x and is close to $2.54\mu_B$/Ce, the value expected for a trivalent Ce ion. However, the paramagnetic Curie temperature θ_P decreases from 12 K for $x=0$ to 0 K for $x=0.4$. The low-temperature data of $\chi(T)$ are shown in the inset of Fig. 1. For $x=0$, $\chi(T)$ exhibits a sharp peak at $T_N = 16$ K followed by a minimum at 10 K, below which an AF phase of the type IA is stabilized.[4] For $x \geqslant 0.05$, $\chi(T)$ is characterized by a broad maximum, of which temperature was taken as T_N, because it agrees with an anomaly in $\rho(T)$.

Temperature variations of $\rho(T)/\rho(300\,\text{K})$ are represented in Fig. 1. Because of the presence of microcracks, the data

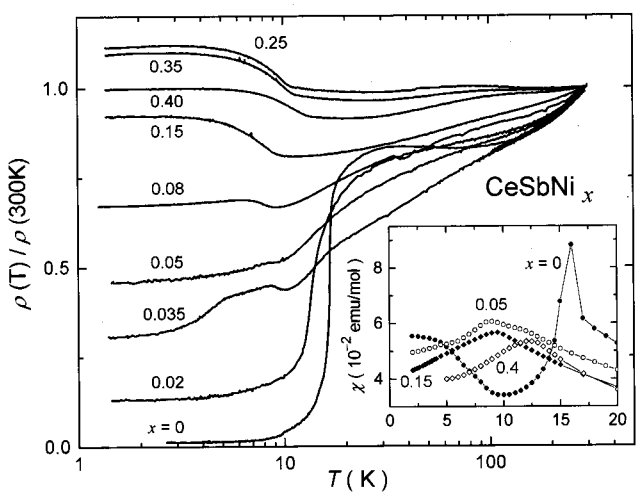

FIG. 1. Temperature dependence of electrical resistivity $\rho(T)$ for polycrystalline samples of $CeSbNi_x$ ($0 \leqslant x \leqslant 0.4$). The data are normalized to the value at 300 K. The inset shows the magnetic susceptibility measured in a field of 0.5 T.

are normalized to the room-temperature value. Typical values at 300 K are 150 and 560 $\mu\Omega$ cm for $x=0$ and 0.4, respectively. As the temperature is lowered, $\rho(T)$ for $x=0$ passes through a broad maximum at 30 K and drops suddenly at $T_N=16$ K. For $x \leqslant 0.05$, $\rho(T)$ decreases on cooling, while that for $x \geqslant 0.08$ increases just below T_N. The sharp rise found for $x=0.15$ is tentatively ascribed to an AF superzone gap. If this is the case, the gap should be suppressed when the AF order is destroyed by a sufficiently high magnetic field. To confirm this supposition, we measured the resistivity as the functions of T and B for the single crystal with $x=0.15$.

The inset of the upper panel of Fig. 2 shows the results of $\rho(T)$ for $B \| I \| [100]$. As expected, the sharp rise in $\rho(T)$ below T_N is suppressed on increasing the applied field, concomitant with the decrease of T_N. In fields above 10 T, no anomaly is noticed down to 1.3 K. It is noteworthy that these effects are very similar for two configurations, $B \| I \| [100]$ and $B \perp I \| [100]$ (not shown in Fig. 2). This observation is consistent with the absence of magnetic anisotropy for $x=0.15$.[15] Another interesting observation is the different behavior between the zero-field cooled (ZFC) and field cooled (FC) data. It is assumed that the ZFC state consists of many AF domains, while the FC state may have mono domain with Ce magnetic moments parallel to the direction of applied field if the anisotropy energy is sufficiently low. The different domain structures may cause the observed variations in the zero-field data.

The close relation between the magnetoresistance $\rho(B)$ and the magnetization $M(B)$ for $B \| [100]$ is demonstrated in Fig. 2. We observed that the virgin curves of $\rho(B)$ for $B \| I$ and $B \perp I$ at 1.5 K show a sudden jump and a drop at 1.7 T, respectively. The $M(B)$ curve also exhibits a weak hysteresis at the same field, as is noticed in the inset of the lower panel of Fig. 2. Therefore the anomalies in $\rho(B)$ at 1.7 T is ascribed to the effect of reorientation of domains, as mentioned above. With a further increase of field up to 5 T, both $\rho(B \| I)$ and $\rho(B \perp I)$ decrease significantly and $d\rho/dB$ has the maximum at $B=6.5$ T. This field value agrees with the

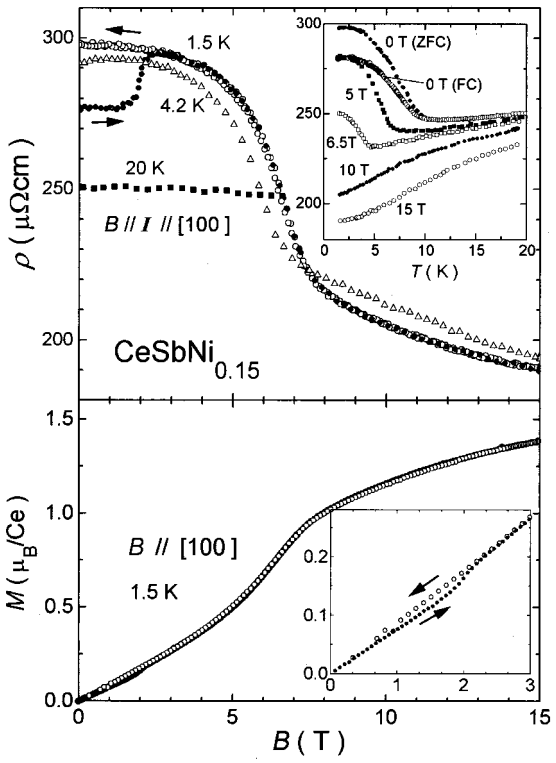

FIG. 2. Upper panel: magnetic-field dependence of resistivity $\rho(B)$ for the single crystal $CeSbNi_{0.15}$ at various temperatures for $B \| I \| [100]$. The inset shows $\rho(T)$ in several constant magnetic fields. Lower panel: magnetization $M(B)$ of $CeSbNi_{0.15}$ at 1.5 K. The inset shows the low-field data of $M(B)$.

metamagnetic-transition field in $M(B)$. Therefore we may conclude that the superzone gap is eliminated by the metamagnetic transition from the AF state to a field-induced ferromagnetic state.

The dependence of $M(B)$ on x was studied by using polycrystalline samples of $CeSbNi_x$ ($0 \leqslant x \leqslant 0.4$). Figure 3 shows the $M(B)$ curves at 4.2 K up to 15 T. $M(B)$ for $x=0$ exhibits a strong hysteresis with two metamagnetic transitions at 2 and 4 T, as reported previously,[5] and the saturation moment of $1.85\mu_B$/Ce equals the average value reported for $B \| [100]$, [110], and [111].[5] With increasing x up to 0.05, the metamagnetic behavior with hysteresis is weakened but the saturation moment is unchanged. For $x=0.08$, however, both the hysteresis and the metamagnetic transition at 2 T disappear. The saturation is not achieved in the highest field of 15 T, where $M(B)$ reaches a value of about $1.2\mu_B$/Ce. No significant change in the $M(B)$ curve occurs with further increase of x to 0.4. The measurement of $M(B)$ up to 55 T for $x=0.15$ indicated that $M(B)$ at 4.2 K gradually increases to $2\mu_B$/Ce.

To examine the change of carrier concentration in $CeSbNi_x$ with x, we measured the Hall coefficient $R_H(T)$. In Fig. 4, the data for the single crystal $CeSbNi_{0.15}$ are compared with that reported for CeSb.[16] The absolute value of $R_H(T)$ for $CeSbNi_{0.15}$ is approximately half that for CeSb. This fact suggests that the electron-carrier concentration is increased by the Ni incorporation. The Hall effect in the paramagnetic state is generally analyzed by using the empirical ansatz, $R_H(T)=R_0+4\pi\chi(T)R_S$, where R_0 and R_S are the normal and anomalous Hall coefficients.[17] However, it

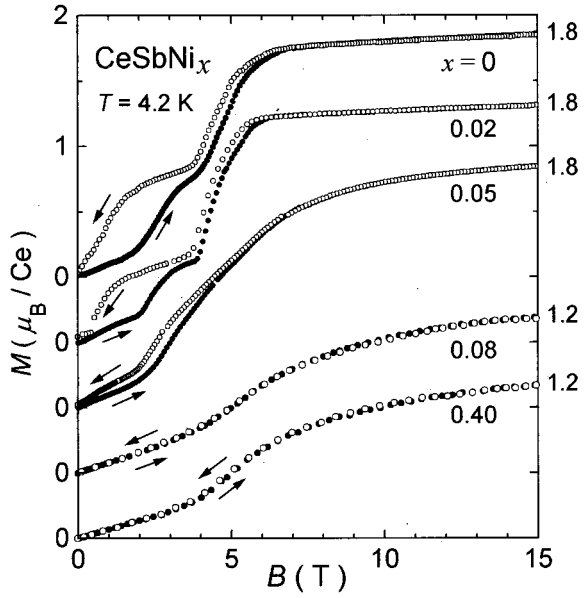

FIG. 3. Magnetization curves for polycrystalline samples of $CeSbNi_x$ ($0 \leqslant x \leqslant 0.4$) at 4.2 K upon increasing and decreasing magnetic field.

was reported that this equation cannot describe the data for CeSb.[16] On the other hand, the fit to the data for $CeSbNi_{0.15}$ is rather good as is shown by the solid line, which gives the values of $R_0 = -5.08 \times 10^{-3}\,\mathrm{cm^3/C}$ and $R_S = +1.17 \times 10^{-3}\,(\mathrm{cm^3/C})/(\mathrm{emu/mol})$. The semimetallic nature does not allow us to estimate the carrier concentration solely from the value of R_0. In the inset of Fig. 4, the strong increase of $|R_H(T)|$ just below $T_N = 9.5\,\mathrm{K}$ coincides with the rapid rise in $\rho(T)$. This fact indicates the sudden loss of the carriers due to the formation of the superzone gap.

The data for $CeSbNi_x$ ($0 \leqslant x \leqslant 0.4$) obtained by the present studies are summarized in Fig. 5; the cubic lattice parameter a, paramagnetic Curie temperature θ_P, magnetization M at $B = 15\,\mathrm{T}$, and Néel temperature T_N as a function of x. In the lowest panel, the crystal-field splitting Δ obtained

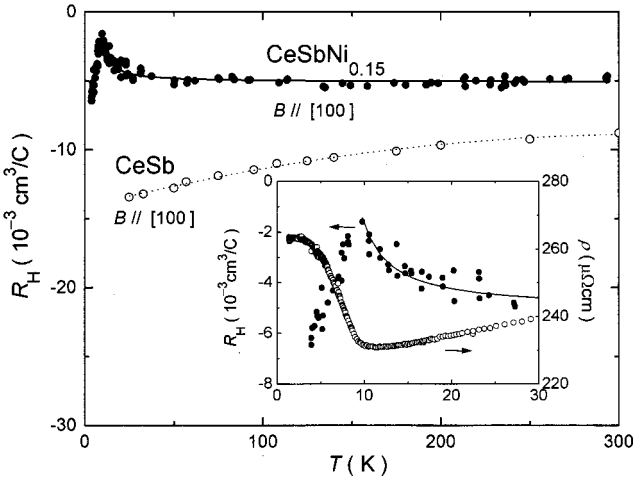

FIG. 4. Temperature dependence of Hall coefficient $R_H(T)$ for the single crystal $CeSbNi_{0.15}$. The solid line represents the best fit (see text). The data of CeSb are taken from Ref. 16. The data of $R_H(T)$ and $\rho(T)$ for $CeSbNi_{0.15}$ are compared in the inset.

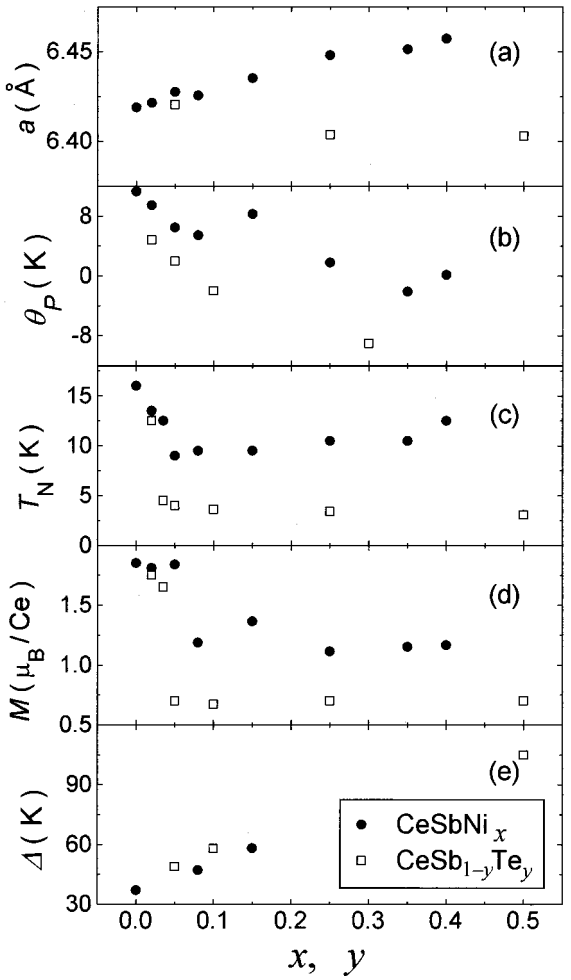

FIG. 5. (a) Cubic lattice parameter a, (b) paramagnetic Curie temperature θ_P, (c) Néel temperature T_N, (d) magnetization M at 15 T, and (e) crystal-field splitting Δ for $CeSbNi_x$ and $CeSb_{1-y}Te_y$ as a function of x and y, respectively. The data for $CeSb_{1-y}Te_y$ are taken from Refs. 7 and 10.

by recent studies of inelastic neutron scattering[18] is shown. Let us now discuss these data by comparing with those reported for $CeSb_{1-y}Te_y$ ($0 \leqslant y \leqslant 0.5$).[7,10] The lattice constant for $CeSbNi_x$ increases almost linearly with x, while that for $CeSb_{1-y}Te_y$ decreases with y. Nevertheless, the traces of θ_P, M, T_N, and Δ are similar as the functions of x and y, respectively. In fact, both T_N and M for $CeSbNi_x$ and $CeSb_{1-y}Te_y$ strongly decrease in such a small concentration range, $x \leqslant 0.05$ and $y \leqslant 0.05$. The magnetic anisotropy in CeSb disappears for $x > 0.05$ and $y > 0.05$, where the type-I ground state is stabilized.[1,18] The anomalous effects in $CeSb_{1-y}Te_y$ were explained as follows. The substitution of Te for Sb adds the $5p$ electrons which fill the $5p$-hole band, and thus weakens the p-f mixing. This collapse of p-f mixing strongly depresses T_N and increases Δ.[10] In $CeSbNi_x$, the $3d$ state of Ni may overlap with the $5p$ band of Sb, and then reduce the $5p$-hole concentration. This results in similar collapse of p-f mixing as in $CeSb_{1-y}Te_y$.

In order to understand the mechanism of the collapse of p-f mixing, we should recall the unique magnetic structure of CeSb in the ground state. The ferromagnetically coupled double layers are stacked antiferromagnetically along the [100] direction with the sequence $(++--)$.[4] The competi-

tion of ferromagnetic and AF couplings between the ferromagnetic layers have recently been explained by considering intraband (ferromagnetic) and interband (AF) exchange interactions between the localized $4f$ spins and two types of carriers.[19] Following this model, we discuss now why both T_N and M in $CeSbNi_x$ and $CeSb_{1-y}Te_y$ strongly decrease for such small amounts of Ni and Te, $x \leqslant 0.05$ and $y \leqslant 0.05$. In both systems, the reduction of $5p$-hole concentration should weaken both the intraband and interband interactions, as described below. The intraband interaction is proportional to the square of the *p-f* mixing interaction, whereas the interband one is to the product of the *p-f* mixing and the *d-f* mixing.[19] As the *p-f* mixing is reduced with the Ni incorporation, the intraband ferromagnetic interaction is more strongly weakened than the interband AF one. This argument is supported by the steady decrease of θ_P with x, as was shown in Fig. 5(b). When the AF interaction dominates the ferromagnetic one, the double ferromagnetic layers are destabilized and instead the type-I ground state is realized in $CeSbNi_x$ ($x \geqslant 0.08$) (Ref. 18) and $CeSb_{1-y}Te_y$ ($y \geqslant 0.05$).[1]

Next, we discuss the reason for the opposite change in $\rho(T)$ below T_N for $CeSbNi_x$ and $CeSb_{1-y}Te_y$. Below T_N, $\rho(T)$ for $x \geqslant 0.08$ increases abruptly but that for $y \geqslant 0.05$ decreases, although both undergo the transition into the type-I AF phase. It should be recalled that the Fermi surface of CeSb consists of the Sb $5p$-hole bands centered at Γ point and Ce $5d$-electron bands centered at X point.[20,21] The electron bands are mostly responsible for the electrical conductivity because the mobility of electrons is much higher than that of holes.[16] In $CeSbNi_x$, the effect of addition of Ni $3d$ electrons is not only the decrease of the $5p$-hole concentration but also the increase of the $5d$-electron concentration through the $3d$-$5d$ mixing. Then, the Fermi level of the electron band may across the midpoint between X and Γ points of the first Brillouin zone for CeSb. When the system goes into the type-I AF phase, a superzone boundary is formed at the midpoint due to the doubling of the period of the magnetic lattice. The partial loss of the Fermi surface gives rise to the sharp rise in $\rho(T)$ just below T_N. On the other hand, the effect of substitution of Te for Sb in CeSb is predominantly the decrease in the $5p$-hole concentration. Thereby no significant change would occur in the electron bands, and its Fermi level does not come to the midpoint between X and Γ points. Therefore no superzone gap opens at the Fermi level in the type-I phase of $CeSb_{1-y}Te_y$. When high magnetic field is applied to $CeSbNi_x$, we found that the rapid rise of $\rho(T)$ below T_N for $x \geqslant 0.08$ is quenched by the metamagnetic transition. This indicates that the gap is eliminated by the transition from the type-I AF state to a field-induced ferromagnetic state.

Summing up, we studied the effects of Ni incorporation on the electrotransport and magnetic properties of the low-density carrier system CeSb. The decrease in $|R_H(T)|$ was interpreted as an indication of the decrease in the Sb $5p$-hole concentration. The drastic depression of both T_N and M with x indicates the collapse of *p-f* mixing due to the reduction of $5p$-hole concentration. This collapse is also responsible for the increase of Δ from 37 K for $x=0$ to 58.3 K for $x=0.15$. Furthermore, the magnetic structure changes from the type IA for $x \leqslant 0.05$ to the type I for $x \geqslant 0.08$. Although these facts are analogous to those reported for $CeSb_{1-y}Te_y$, the superzone gap is formed only in the type-I phase of $CeSbNi_x$ for $x \geqslant 0.08$. We therefore propose that the superzone gap is open in the $5d$-electron band at the midpoint between X and Γ points as a result of the increase of the $5d$-electron concentration through the hybridization between Ni $3d$ states and Ce $5d$ states.

We wish to thank F. Iga for valuable advice, and T. Fujita and T. Suzuki for the generous use of their superconducting quantum interference device magnetometer. We thank Y. Shibata for electron-probe microanalysis done at the Instrument Center for Chemical Analysis, Hiroshima University. The Hall-effect measurements were performed at the Cryogenic Center, Hiroshima University. The authors are also grateful to Y. S. Kwon, M. Sera, H. Nakotte, and N. Shibata for helpful discussions.

*Present address: ISIS Facility, Rutherford Appleton Laboratory, Chilton, Oxon, OX11 OQX, U.K.

[1] J. Rossat-Mignod, J. M. Effantin, P. Burlet, T. Chattopadhyay, L. P. Regnault, H. Bartholin, C. Vettier, O. Vogt, D. Ravot, and J. C. Achart, J. Magn. Magn. Mater. **52**, 111 (1985).

[2] K. Takegahara, H. Takahashi, A. Yanase, and T. Kasuya, Solid State Commun. **39**, 857 (1981).

[3] N. Kioussis, B. R. Cooper, and J. M. Wills, Phys. Rev. B **44**, 10 003 (1991).

[4] J. Rossat-Mignod, P. Burlet, J. Villain, H. Bartholin, T. S. Wang, D. Florence, and O. Vogt, Phys. Rev. B **16**, 440 (1977).

[5] G. Busch and O. Vogt, Phys. Lett. **25A**, 449 (1967).

[6] B. D. Rainford, K. C. Turberfield, G. Busch, and O. Vogt, J. Phys. C **1**, 679 (1968).

[7] H. Bartholin, J. M. Effantin, P. Burlet, J. Rossat-Mignod, J. C. Achart, and D. Ravot, J. Magn. Magn. Mater. **52**, 381 (1985).

[8] T. Chattopadhyay, P. Burlet, J. Rossat-Mignod, H. Bartholin, C. Vettier, and O. Vogt, Phys. Rev. B **49**, 15 096 (1994).

[9] M. Sera, T. Suzuki, and T. Kasuya, J. Magn. Magn. Mater. **31–34**, 385 (1983).

[10] D. Ravot, A. Mauger, J. C. Achard, M. Bartholin, and J. Rossat-Mignod, Phys. Rev. B **28**, 4558 (1983).

[11] J. Rossat-Mignod, P. Burlet, S. Quezel, J. M. Effantin, D. Delacôte, H. Bartholin, O. Vogt, and D. Ravot, J. Magn. Magn. Mater. **31–34**, 398 (1983).

[12] D. Ravot, A. Percheron-Guegan, J. M. Durand, J. Olivier-Fourcade, J. C. Jumas, and P. Parent, J. Alloys Compd. **261**, 12 (1997).

[13] H. Takahashi and T. Kasuya, J. Phys. C **18**, 2697 (1985).

[14] T. Kasuya, Y. Haga, T. Suzuki, Y. Kaneta, and O. Sakai, J. Phys. Soc. Jpn. **61**, 3447 (1992).

[15] D. T. Adroja, M. H. Jung, Y. Shibata, and T. Takabatake, J. Phys.: Condens. Matter **11**, 3687 (1999).

[16] H. Kitazawa, I. Oguro, M. Hirai, Y. Kondo, T. Suzuki, and T. Kasuya, J. Magn. Magn. Mater. **47&48**, 532 (1985).

[17] A. Fert and P. Levy, Phys. Rev. B **36**, 1907 (1987).

[18] D. T. Adroja, J. G. M. Armitage, P. C. Riedi, M. H. Jung, Z. Tun, and T. Takabatake, Phys. Rev. B **62**, 12 181 (2000).

[19] N. Shibata, C. Ishii, and K. Ueda, Phys. Rev. B **52**, 10 232 (1995).

[20] O. Sakai, M. Takeshige, H. Harima, K. Otaki, and T. Kasuya, J. Magn. Magn. Mater. **52**, 18 (1985).

[21] T. Kasuya, O. Sakai, J. Tanaka, H. Kitazawa, and T. Suzuki, J. Magn. Magn. Mater. **63&64**, 9 (1987).